PELLET PARTICLE DEPOSITION PROFILES WITH ALLOWANCE FOR NEUTRAL GAS EXPANSION EFFECTS

P.J. Lalousis*, L.L. Lengyel**

*The NET-Team/IPP Garching
**IPP Garching, EURATOM Association, Fed. Rep. of Germany

A numerical model has been developed recently in which the expansion of the pellet cloud along the magnetic field lines as well as in the transverse direction is calculated by means of a self-consistent model that takes into account such effects as finite rate ionization, $\vec{j} \times \vec{B}$ deceleration, magnetic field convection, and magnetic field diffusion [1]. This model is coupled to a numerical routine in which the local ablation rate is determined as a function of the electron temperature and electron density specified [2]. The total number of particles ablated at a particle flux surface is given by the product of the ablation rate and the residence time of the pellet in the flux tube considered. The expansion and ionization of these particles are followed up numerically until they are stopped at some distance from the pellet. The results of calculations show that the expansion velocity of the neutrals may considerably exceed the traversing velocity of pellets injected into hot plasmas. Hence the neutrals may become ionized and confined to magnetic flux surfaces at some distance from the location of the pellet. The particle deposition profile is thus determined by summing up, at each flux surface, the contributions of particles released by the pellet at the subsequent flux surfaces while traversing them. A numerical algorithm has been developed for this purpose that is described elsewhere [3].

Some representative results corresponding to the injection of single pellets into ASDEX, JET, and NET are given in Figs. 1 to 6. In all these cases the ablation rate was calculated by means of the semi-analytical formula of Ref. [2]:$d\dot{r}_p/dt\alpha Const * T_e^{1.64} * n_e^{0.33}/r_p^{0.67}$. The constant appearing in this expression has been chosen in such a manner as to reproduce the pellet penetration depth experimentally observed in ASDEX (Shot no. 18716). Note that unlimited energy reservoir was assumed in the present calculations, i.e. the finiteness of the flux tube volumes in tokamaks was not taken into account.

In all these figures, the number of particles deposited per flux tube is plotted as a function of the radius. The width of a flux tube is defined (in an arbitrary manner) as $\Delta r = a/40$, 41 being the number of mesh points used in the calculations. The solid lines shown correspond to local particle deposition whereas broken lines to particle

	ASDEX	JET	NET
R (m)	1.65	2.98	5.20
a (m)	0.40	1.20	1.62
B (tesla)	2.2	3.0	5.5
T_{eo} (kev)	30.0	4.58	0.58
T_{e1} (keV)	0.02	0.20	0.20
n_{eo} (m^{-3})	1.5×10^{20}	1.3×10^{19}	1.5×10^{20}
n_{e1} (m^{-3})	0.8×10^{19}	0.5×10^{19}	0.6×10^{19}

In all these cases, the electron temperature and density profiles were prescribed by means of the expression $f(r) = f_1 + (f_0 - f_1)[1 - (r/a)^{EX1}]^{EX2}$, where for T_e EX1 = EX2 = 2 and for n_e EX1 = 2, EX2 = 0.5, respectively.

Figures 1 and 2 correspond to pellet injection into ASDEX with $v_p = 800m/s$. In the reference case (Shot no. 18716, Fig. 1) a pellet of $N_p = 3.2 \times 10^{19}$ ($r_p = 0.5$ mm) has been used. For obtaining deep penetration, a pellet size with $N_p = 5 \times 10^{20}$ has been assumed for Fig. 2. Figure 3 corresponds to pellet injection into JET: here $N_p = 2 \times 10^{21}$ ($r_p = 2$ mm) and $v_p = 1100$ m/s. Figures 4 to 6 correspond to NET scenarios. In the first two cases a rather low pellet velocity, $v_p = 1100m/s$, has been used. The first pellet size, $N_p = 1.6 \times 10^{22}$ ($r_p = 4$ mm, see Fig. 4) corresponds to a NET refuelling pellet [4]. For obtaining intermediate and deep penetrations, the pellet size was increased to $N_p = 7 \times 10^{23}$ and 2×10^{24} (see Figs. 5 and 6, respectively). In the last case, the pellet velocity was increased to 2500 m/s.

The results of these calculations can be summarized as follows:

(a) Within the framework of the analytical (smooth) plasma parameter distributions and the analytical ablation rate function assumed, no notable difference exists between local and non-local particle deposition in the bulk of the plasma. Here non-local deposition has merely a smearing effect.

(b) Non-local deposition may produce notable differences in the wings of the deposition curves particularly at high ablation rates, coupled with limited energy supply.

(c) The existence of significant non-local deposition effects depends upon the amount of the cold mass locally released and the magnitude of the energy flux affecting the neutral cloud. If the resulting ionization process is comperatively slow, significant non-local effects may be produced in the wings of the deposition curves: deeper particle penetration results (see Figs. 2, 5, and 6).

References

[1] See paper P3 A3 46 by L.L. Lengyel and the references cited therein.

[2] P.B. Parks and R.J. Turnbull, Phys. Fluids **21** (1978), 1735.

[3] P.J. Lalousis, An Algorithm for Pellet Particle Deposition with Allowance for Neutral Gas Expansion Effects; see also Lab.-Report (in preparation).

[4] L.L. Lengyel, Fusion Technology **10** (1986) 354.

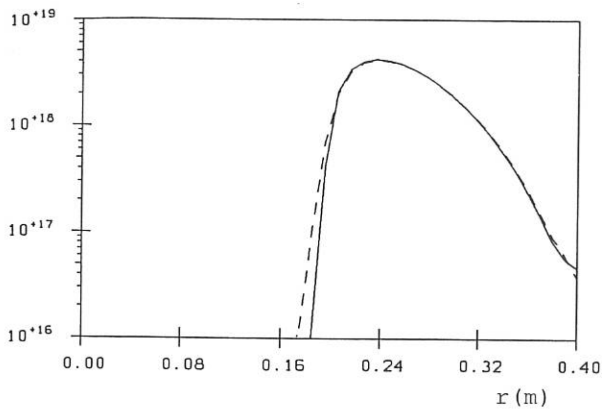

Particle deposition in ASDEX:
$N_p = 3.2 \times 10^{19}$
$v_p = 800$ m/s

Fig. 1

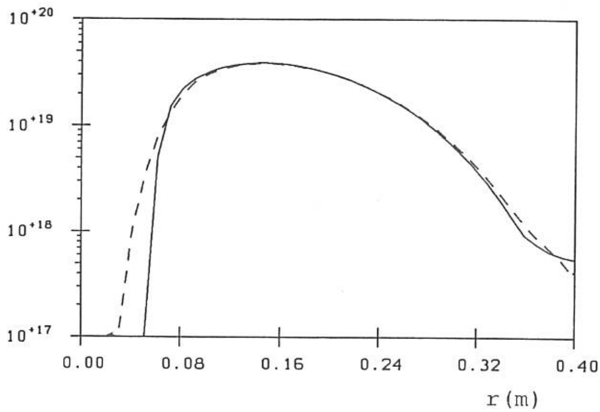

Particle deposition in ASDEX:
$N_p = 5 \times 10^{20}$
$v_p = 800$ m/s

Fig. 2

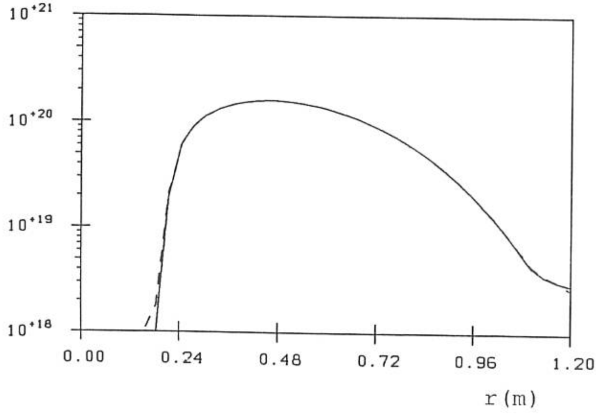

Particle deposition in JET:
$N_p = 2 \times 10^{21}$
$v_p = 1100$ m/s

Fig. 3

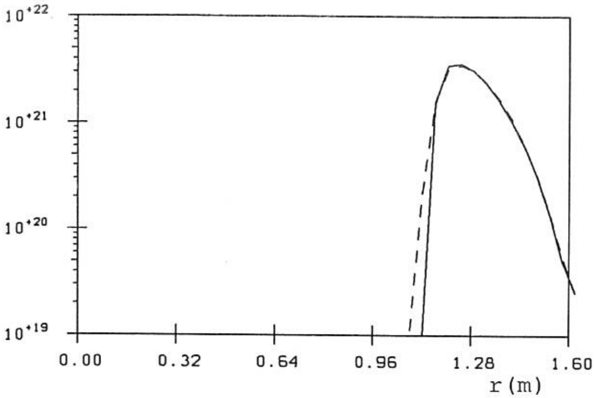

Particle deposition in NET:

$N_p = 1.6 \times 10^{22}$

$v_p = 1100$ m/s

Fig. 4

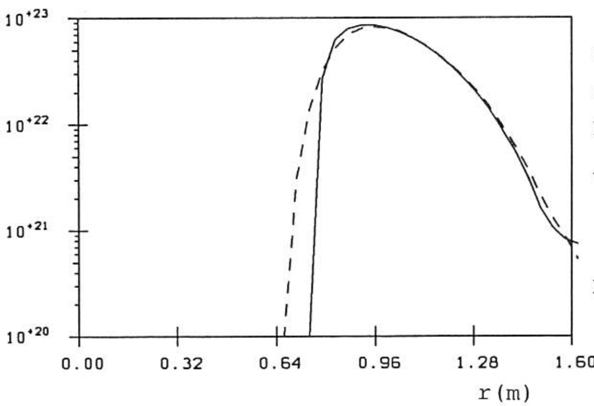

Particle deposition in NET:

$N_p = 7 \times 10^{23}$

$v_p = 1100$ m/s

Fig. 5

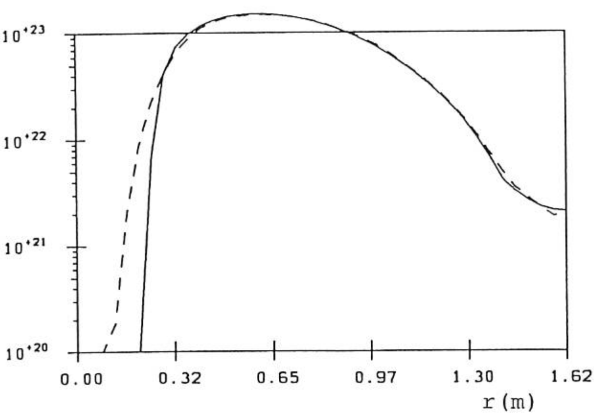

Particle deposition in NET:

$N_p = 2 \times 10^{24}$

$v_p = 2500$ m/s

Fig. 6